10

Supplementary Materials

Global Climate Projections

Coordinating Lead Authors:

Gerald A. Meehl (USA), Thomas F. Stocker (Switzerland)

Lead Authors:

William D. Collins (USA), Pierre Friedlingstein (France, Belgium), Amadou T. Gaye (Senegal), Jonathan M. Gregory (UK), Akio Kitoh (Japan), Reto Knutti (Switzerland), James M. Murphy (UK), Akira Noda (Japan), Sarah C.B. Raper (UK), Ian G. Watterson (Australia), Andrew J. Weaver (Canada), Zong-Ci Zhao (China)

Contributing Authors:

R.B. Alley (USA), J. Annan (Japan, UK), J. Arblaster (USA, Australia), C. Bitz (USA), P. Brockmann (France), V. Brovkin (Germany, Russian Federation), L. Buja (USA), P. Cadule (France), G. Clarke (Canada), M. Collier (Australia), M. Collins (UK), E. Driesschaert (Belgium), N.A. Diansky (Russian Federation), M. Dix (Australia), K. Dixon (USA), J.-L. Dufresne (France), M. Dyurgerov (Sweden, USA), M. Eby (Canada), N.R. Edwards (UK), S. Emori (Japan), P. Forster (UK), R. Furrer (USA, Switzerland), P. Gleckler (USA), J. Hansen (USA), G. Harris (UK, New Zealand), G.C. Hegerl (USA, Germany), M. Holland (USA), A. Hu (USA, China), P. Huybrechts (Belgium), C. Jones (UK), F. Joos (Switzerland), J.H. Jungclaus (Germany), J. Kettleborough (UK), M. Kimoto (Japan), T. Knutson (USA), M. Krynytzky (USA), D. Lawrence (USA), A. Le Brocq (UK), M.-F. Loutre (Belgium), J. Lowe (UK), H.D. Matthews (Canada), M. Meinshausen (Germany), S.A. Müller (Switzerland), S. Nawrath (Germany), J. Oerlemans (Netherlands), M. Oppenheimer (USA), J. Orr (Monaco, USA), J. Overpeck (USA), T. Palmer (ECMWF, UK), A. Payne (UK), G.-K. Plattner (Switzerland), J. Räisänen (Finland), A. Rinke (Germany), E. Roeckner (Germany), G.L. Russell (USA), D. Salas y Melia (France), B. Santer (USA), G. Schmidt (USA, UK), A. Schmittner (USA, Germany), B. Schneider (Germany), A. Shepherd (UK), A. Sokolov (USA, Russian Federation), D. Stainforth (UK), P.A. Stott (UK), R.J. Stouffer (USA), K.E. Taylor (USA), C. Tebaldi (USA), H. Teng (USA, China), L. Terray (France), R. van de Wal (Netherlands), D. Vaughan (UK), E. M. Volodin (Russian Federation), B. Wang (China), T. M. L. Wigley (USA), M. Wild (Switzerland), J. Yoshimura (Japan), R. Yu (China), S. Yukimoto (Japan)

Review Editors:

Myles Allen (UK), Govind Ballabh Pant (India)

This chapter should be cited as:

Meehl, G.A., T.F. Stocker, W.D. Collins, P. Friedlingstein, A.T. Gaye, J.M. Gregory, A. Kitoh, R. Knutti, J.M. Murphy, A. Noda, S.C.B. Raper, I.G. Watterson, A.J. Weaver and Z.-C. Zhao, 2007: Global Climate Projections. In: *Climate Change 2007: The Physical Science Basis. Contribution of Working Group I to the Fourth Assessment Report of the Intergovernmental Panel on Climate Change* [Solomon, S., D. Qin, M. Manning, Z. Chen, M. Marquis, K.B. Averyt, M. Tignor and H.L. Miller (eds.)]. Cambridge University Press, Cambridge, United Kingdom and New York, NY, USA.

Contents

Details of data preparation for runoff and soil moisture plots (Fig. 10.12)

For both these land quantities a technique was used to allow improved presentation of the simulated data, particularly at coasts. The basic method was previously used for the soil moisture plot of the Working Group I contribution to the IPCC Second Assessment Report (Figure 6.12). Firstly, for each model, each climatological field was tested for data that were clearly invalid, including missing values over ocean and ice sheets. Data outside the range 10^{-12} and 0.001 kg m^{-2} s^{-1} for runoff, and 10^{-4} and 3000 kg m^{-2} for soil moisture, were set to a missing value. The field was then interpolated to a finer grid with halved spacing, letting valid data extend to the original coastlines. The resulting field from each model was then interpolated to a common fine grid. At each point, a simple average was then used, provided there were valid data from at least 10 models. This produced a field with data for most of the true land, and excluding permanent ice sheets in the case of soil moisture. Land with seasonal cover may still be poorly represented by this process. For soil moisture the field plotted was the change as a percentage of the multi-model mean for 1980-1999. In effect, the changes were biased towards those in models with a greater depth of soil, but this is not unreasonable given that these are likely more sophisticated schemes. Averaging the individual percentage changes produced a noisier field. The use of normalised soil moisture changes by Wang (2005) is a worthy alternative.

Table S10.1. Models used in constructing multi-model means shown in figures in Section 10.3. Letters below figure numbers refer either to the SRES scenario considered or to the panel within the figure.

	Figure[a]													
	10.6	10.7	10.8			10.9	10.10		10.11		10.12			
Model			(B1)	(A1B)	(A2)		(a)	(b)	(a)	(b)	(a)	(b)	(c)	(d)
BCCR-BCM2.0			X		X									
CCSM3	X	X	X	X	X	X	X	X	X	X	X	X	X	X
CGCM3.1(T47)	X	X	X	X	X	X	X	X	X	X	X	X	X	X
CGCM3.1(T63)		X	X	X		X	X	X	X	X	X	X	X	X
CNRM-CM3	X	X	X	X	X	X		X	X	X	X			X
CSIRO-MK3.0	X	X	X	X	X	X		X	X	X	X			X
ECHAM5/MPI-OM			X	X	X	X		X	X	X	X	X	X	X
ECHO-G	X		X	X	X	X		X	X	X	X	X	X	X
FGOALS-g1.0		X	X		X	X	X	X	X	X	X	X	X	X
GFDL-CM2.0	X	X	X	X	X	X	X	X	X	X	X	X	X	X
GFDL-CM2.1	X		X	X	X	X	X	X	X	X	X	X	X	X
GISS-AOM			X	X		X		X		X	X	X	X	X
GISS-EH		X		X		X	X	X	X		X	X	X	X
GISS-ER	X		X	X	X	X	X	X	X	X	X	X	X	X
INM-CM3.0	X		X	X	X	X	X	X	X	X	X	X	X	X
IPSL-CM4	X	X	X	X	X	X	X	X	X	X	X	X	X	X
MIROC3.2 (hires)			X	X		X		X	X	X	X	X	X	X
MIROC3.2 (medres)	X		X	X	X	X	X	X	X	X	X	X	X	X
MRI-CGCM2.3.2	X	X	X	X	X	X		X	X	X	X	X	X	X
PCM	X	X	X	X	X	X	X	X	X		X	X	X	X
UKMO-HadCM3	X	X	X	X	X	X	X	X	X		X	X	X	X
UKMO-HadGEM1				X	X	X		X	X		X	X	X	X

[a] Note Section 10.3 figure contents are as follows:
Figure 10.6: zonal average temperature and precipitation
Figure 10.7: atmospheric and oceanic temperature
Figure 10.8: surface air temperature
Figure 10.9: seasonal temperature, rainfall, sea level pressure
Figure 10.10a: zonal average cloud fraction
Figure 10.10b: total cloud fraction
Figure 10.11a: cloud radiative forcing
Figure 10.11b: diurnal temperature range
Figure 10.12: precipitation, soil moisture, runoff, evaporation

Table S10.2. Global mean change in annual mean precipitation from the multi-model ensemble mean for four time periods relative to 1980–1999, for each of the available scenarios. Values are given as a percentage of the global mean for 1980-1999 (2.83 mm d^{-1}), divided by the global mean warming for each case (Table 10.5). (The data are averages of the series depicted in Fig. 10.5.) Also given are two measures of agreement of the geographic scaled patterns of change (the precipitation fields normalised by the global mean warming), relative to the A1B 2080–2099 case. First the non-dimensional M value (see text, and caption to Table 10.5), and second (in italics) the mae (global mean absolute 'error'or difference, in ***mm d*** $^{-1}$ *K^{-1}) between the fields, both multiplied by 100 for brevity. 'Commit' refers to the constant-composition commitment experiment.*

	Global mean rainfall change (scaled, % K^{-1})				Measures of agreement of scaled field (M × 100 n.d., mae × 100 mm d^{-1} K^{-1})			
	2011–2030	2046–2065	2080–2099	2180–2199	2011–2030	2046–2065	2080–2099	2180–2199
A2	1.38	1.33	1.45		56, 5	80, 2	84, 2	
A1B	1.45	1.51	1.63	1.68	66, 4	86, 2	100, 0	86, 2
B1	1.62	1.65	1.88	1.89	68, 4	80, 2	84, 2	80, 2
Commit	2.27	2.32	2.29		46, 7	55, 6	57, 5	

Supplementary Figure S10.1. *Multi model mean snow cover and projected changes over the 21st century from 12 (a and b) and 11 (c) AOGCMs, respectively. a) Contours mark the locations where the December to February (DJF) snow area fraction exceeds 50%, blue for the period 1980–1999, and red for 2080–2099, dashed for the individual models and solid for the multi model mean. b) Projected multi model mean change in snow area fraction over the period 2080–2099, relative to 1980-1999. Shading denotes regions where the ensemble mean divided by the ensemble standard deviation exceeds 1.0 (in magnitude), c) as b) but changes in snow depth (in cm).*

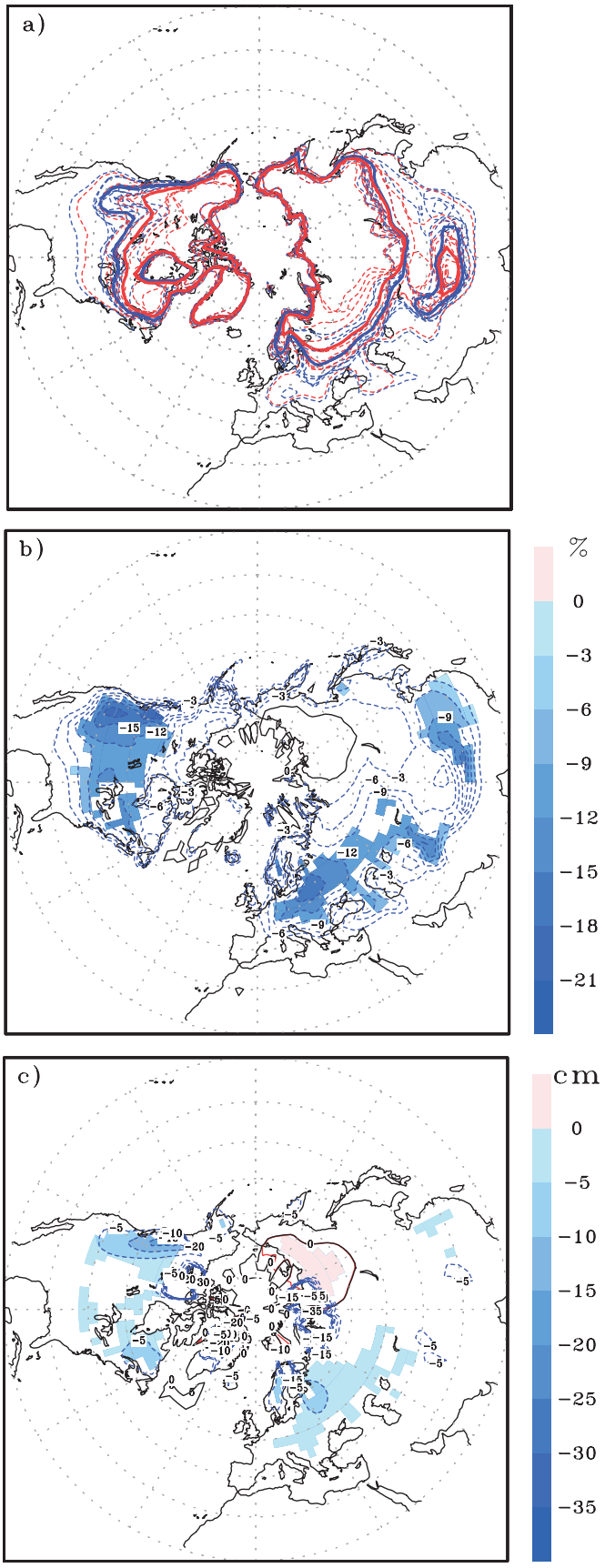

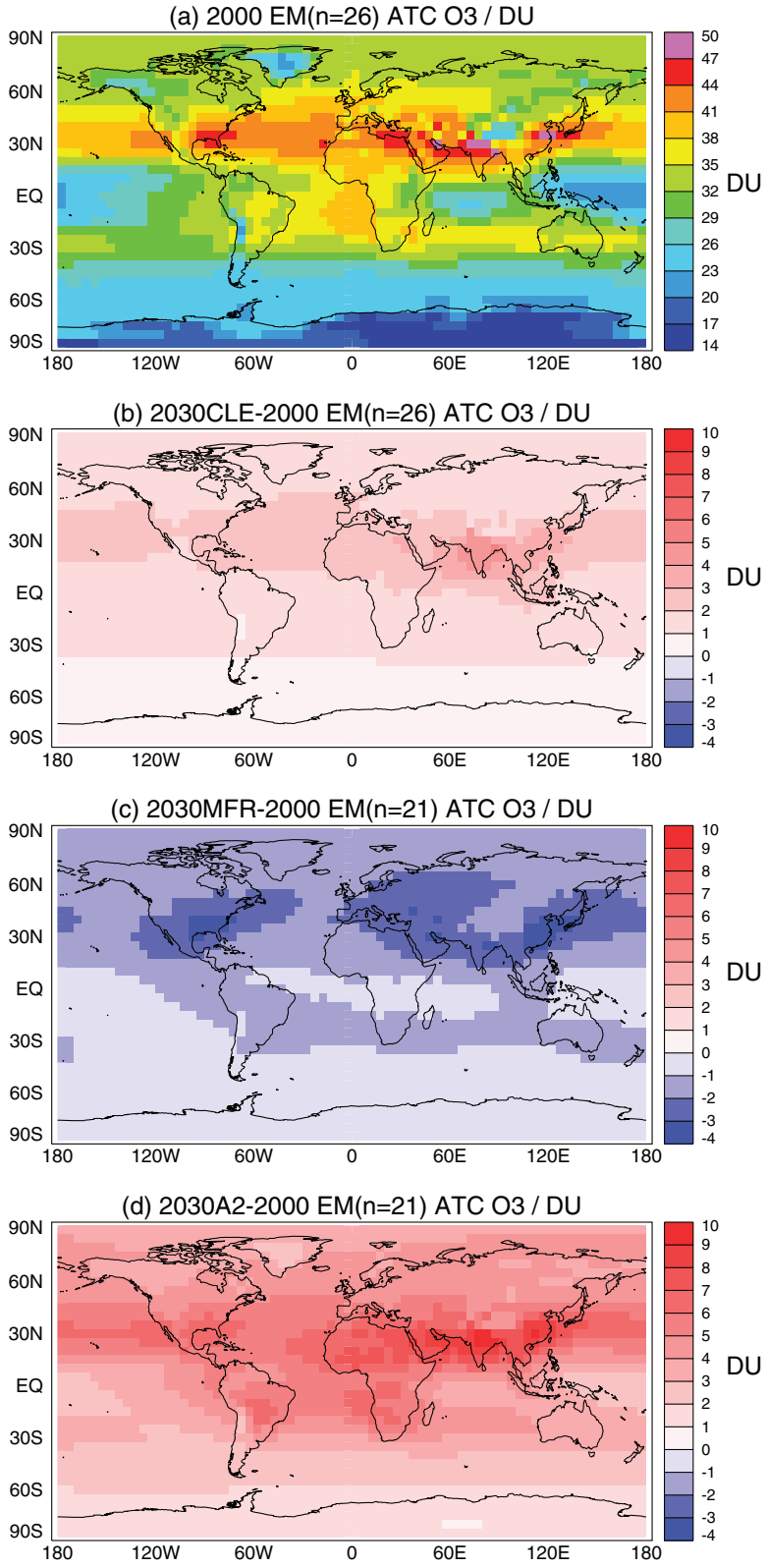

Supplementary Figure S10.2. Tropospheric ozone simulated in the ACCENT model intercomparison (Stevenson et al., 2006). The panels in the figure show annual mean tropospheric column results (in units of DU). Each panel is a multi model ensemble mean; the number of models in the ensemble is given in brackets. (a) Year 2000; (b) difference between 2030CLE (IIASA Current Legislation) scenario and 2000; (c) difference between 2030MFR (IIASA Maximum Feasible Reductions) and 2000; and (d) difference between 2030A2 (SRES A2) and 2000.

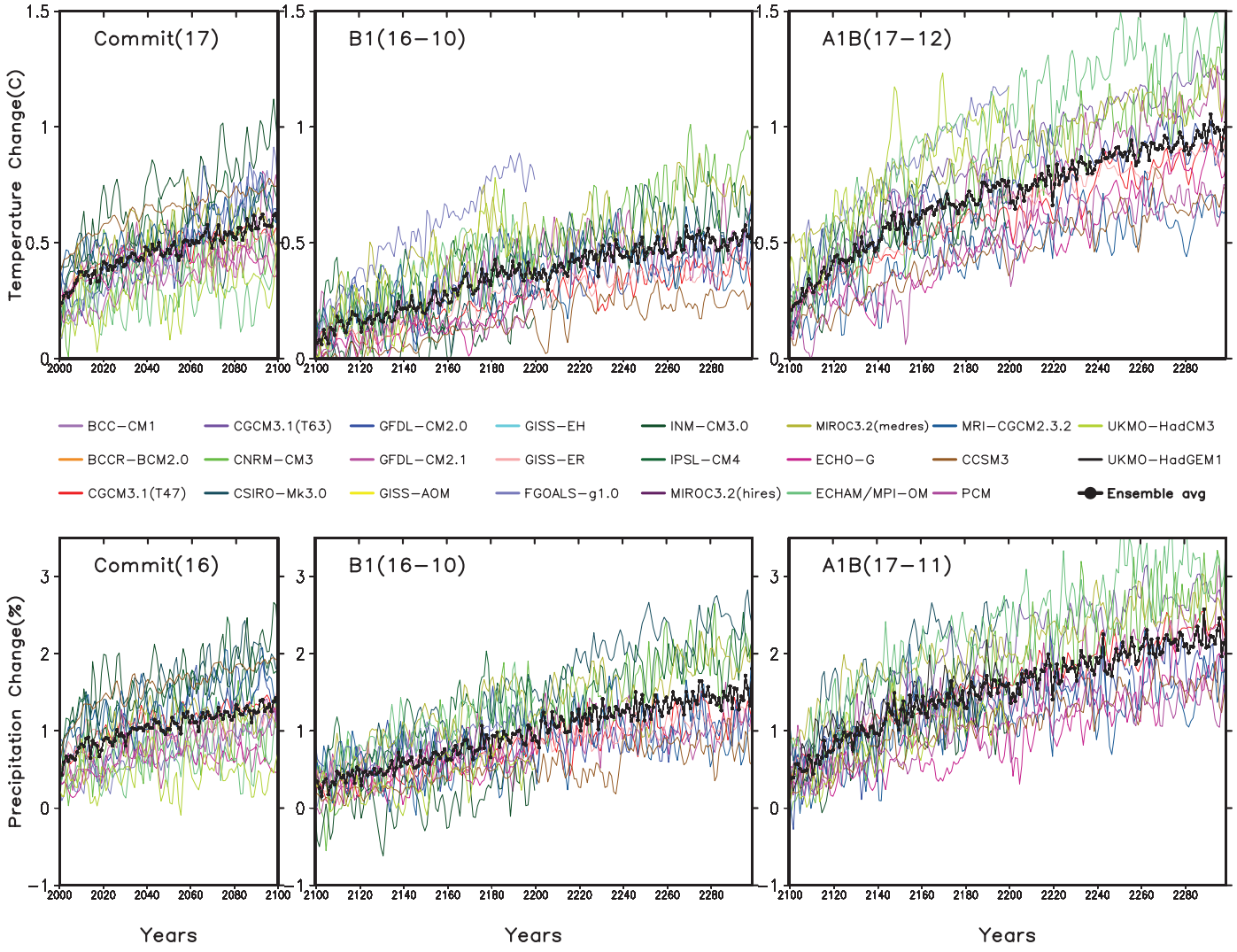

Supplementary Figure S10.3. *Top left: Globally averaged surface air temperature change relative to 1980–1999 for the 20th century commitment experiment; Top center: Same as left except for the B1 commitment experiment computed with respect to the 2080–2099 average; Top right: Same as center except for the A1B commitment experiment; Bottom row: same as top row but for percent change in globally averaged precipitation. The numbers in the panels denote the number of models used for each scenario and each century.*

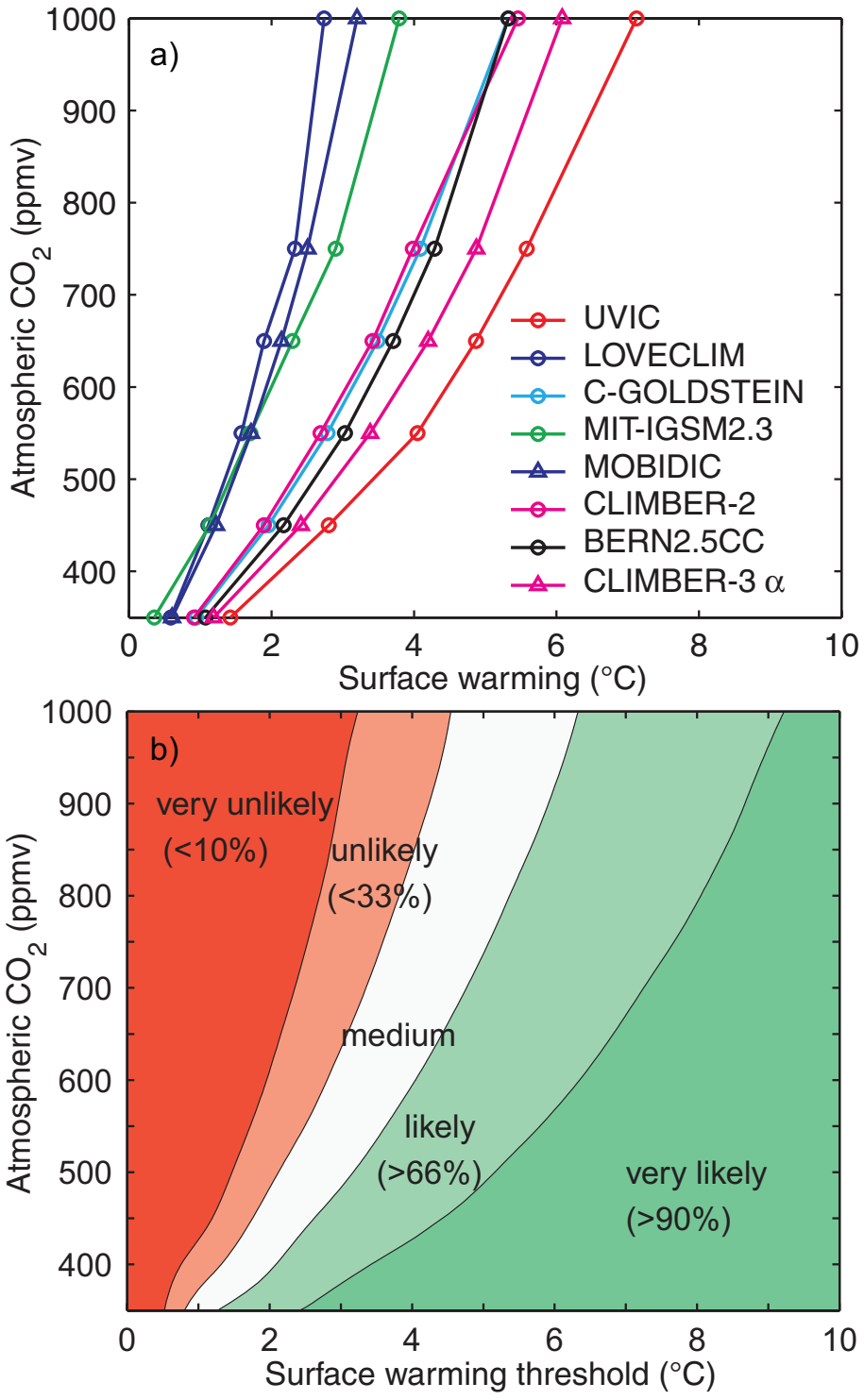

Supplementary Figure S10.4. *a) Equilibrium surface warming for seven different EMICs and different stabilization levels of atmospheric CO_2 or the equivalent radiative forcing, b) a probabilistic picture based on the same scenarios, showing probability of remaining below a certain warming threshold for a given CO_2-equivalent stabilization concentration, derived from Bern2.5D EMIC with variable ocean heat uptake and using several PDFs of climate sensitivity (modified from Knutti et al. (2005)).*